Tunneling-induced π-phase shift with a single-photon signal field in asymmetric double quantum wells

Hongju Guo (郭洪菊)[1,2], Lichun Wang (汪丽春)[1,2], Yueping Niu (钮月萍)[1], Shiqi Jin (金石琦)[1*], and Shangqing Gong (龚尚庆)[1]

[1] *State Key Laboratory of High Field Laser Physics, Shanghai Institute of Optics and Fine Mechanics, Chinese Academy of Sciences, Shanghai 201800, China*

[2] *Graduate University of Chinese Academy of Sciences, Beijing 100049, China*

[*] *E-mail: sqjin@mail.shcnc.ac.cn*

Received April 13, 2009

A theoretical investigation is carried out into the cross phase modulation (XPM) in an asymmetric double AlGaAs/GaAs quantum wells structure with a common continuum. It is found that, combining resonant tunneling-induced transparency and constructive interference in the third-order Kerr effect, a giant XPM can be achieved with vanishing linear and nonlinear absorptions, accompanied by the velocities of the probe and signal fields being matched. Furthermore, this giant XPM could induce a π-phase shift at a single-photon level which is favorable for the applications in two-qubit quantum logic gates.

OCIS codes: 190.3270, 190.4400, 270.1670, 270.5585.

doi: 10.3788/COL20090710.0886.

In the past few decades, there have been tremendous interests in the study of cross phase modulation (XPM). An efficient XPM is useful in many possible applications, such as optical communications[1−3], optical Kerr shutters[4], and quantum phase gates[5]. Especially, a large XPM is desirable for low pump powers and light sensitivities. In order to obtain a large XPM, many studies aiming at the steep dispersion associated with narrow electromagnetically induced transparency (EIT) have been proposed. In a four-level *N*-configuration system, using EIT, the conditional phase shift in XPM has been dramatically improved by several orders of magnitude[6]. In a quasi-three-level scheme, the enhanced third-order susceptibility could be achieved through the autoionizing resonance, in which coherence is established essentially by nonradiative interactions[7]. While, in practical applications, solid materials are more adaptive due to their high electron density, large electric dipole moment, little volume, and ease to control. For such a reason, recently, these studies have been vastly extended to semiconductors for the possible implementation of optical devices because the confined electron gas in a conduction band of semiconductor quantum structure can exhibit atomic-like properties, for example, strong EIT[8], tunneling-induced transparency (TIT)[9], ultrafast all-optical switching[10], slow light[11], etc. The work of Nakajima[7] has been extended into an asymmetric double GaAs quantum wells (QWs) structure and the enhanced Kerr nonlinearity has been achieved[12]. Very recently, in an asymmetric double AlGaAs/GaAs QWs structure with a continuum[13], large XPM has been generated owing to resonant tunneling and Fano interference[14], which leads to a π XPM phase shift under a 300-photon control field.

It is well known that, in quantum information processing, if the nonlinear phase shifts arising from such a XPM are on the order of π rad, it would be possible to implement all-optical switching. Moreover, if the nonlinear phase shifts are obtained on the single-photon level, it could be further used to implement two-qubit quantum logic gates[15]. However, the main impediment towards their operation at few-photon level is the weakness of optical nonlinearities in conventional media[4]. The main hindrance of such schemes is the mismatch between the group velocities of the pulses subject to EIT and their nearly free propagating partners, which severely limits their efficient interaction length[16]. In view of this point, the Kerr nonlinear coupling between two components of the probe was studied, where a novel regime or symmetric, extremely efficient XPM, capable of fully entangling two single-photon pulses was demonstrated[17]. An *M*-scheme as a promising source of giant nonlinearities was also proposed in which two different light-atom configurations were considered, their efficiency in generating large nonlinear cross phase shifts were compared, and the conditions leading to group velocity matching for two light fields were identified[18]. Furthermore, a XPM using single-photon pulses with matched group velocities was considered in a four-level atomic system in which the presence of an optical thick medium was essential for large photon-photon interaction[19]. The maximum phase shift of 0.1 rad has been estimated for Gaussian pulses at single-photon level under realistic conditions for ^{87}Rb with matched group velocities for two interacting pulses[20]. Also, in an atomic system, a π-phase shift was obtained for an all-switching quantum phase gate that used traveling single-photon pulses[21]. Experimentally, phase shifts up to $\pi/4$ have been observed in the coupling of a single quantum dot with a photonic crystal nanocavity controlled by two modes of light at the single-photon level[22].

In this letter, enlightened by the work above, we investigate the XPM which induces a π cross nonlinear phase shift on the level of single-photon in an n-doped asymmetric AlGaAs/GaAs double QWs structure. In this structure, quantum tunneling to a continuum from two resonant excited levels could give rise to Fano-type

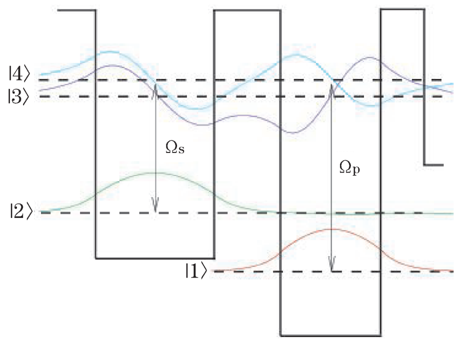

Fig. 1. Conduction subbands of the asymmetric double QWs structure.

interference, which will lead to transparency. Combining this resonant TIT with constructive interference in nonlinear susceptibility, a giant XPM is achieved with vanishing linear and nonlinear absorptions. Via initially prepared population on both low-lying subbands, the condition of group velocity matching between the signal and probe fields is satisfied in the transparent point, which guarantees an efficient interaction length. More importantly, under the conditions of matched velocities and proper parameters, this giant XPM could induce a π-phase shift at the single-photon level.

The n-doped asymmetric AlGaAs/GaAs double QWs structure with the relevant conduction band energy levels and wave functions is shown in Fig. 1. An $\mathrm{Al_{0.07}Ga_{0.93}As}$ layer with the thickness of 8.3 nm is separated from a 6.9-nm GaAs layer by a 4.8-nm $\mathrm{Al_{0.32}Ga_{0.68}As}$ potential barrier. On the right side of the right well, there is a thin (3.4 nm) $\mathrm{Al_{0.32}Ga_{0.68}As}$ barrier, which is followed by a thick $\mathrm{Al_{0.16}Ga_{0.84}As}$ layer. In this structure, one would observe the ground subbands $|1\rangle$ and $|2\rangle$ with energies of 51.53 and 97.78 meV, respectively. Two closely spaced delocalized upper levels $|3\rangle$ and $|4\rangle$ are created by mixing the excited subband of the shallow well $|\mathrm{se}\rangle$ and the excited subband of the right deep well $|\mathrm{de}\rangle$ by tunneling, and they have energies of 191.30 and 203.06 meV, respectively. The solid curves represent the corresponding wave functions. A coherent pulse (probe) with the central frequency ω_p couples the ground level $|1\rangle$ to the excited levels $|3\rangle$ and $|4\rangle$, while another coherent pulse (signal) with the central frequency ω_s couples the intermediate level $|2\rangle$ with two excited levels.

For this semiconductor structure, electrons in upper levels $|3\rangle$ and $|4\rangle$ rapidly decay to the same continuum by tunneling through the thin barrier adjacent to the deep well with rates γ_3^ph and γ_4^ph, respectively. A Fano-type quantum interference arising from this is described by the cross-coupling term $\gamma_{34} = \sqrt{\gamma_3^\mathrm{ph}\gamma_4^\mathrm{ph}}$ [7,21]. Besides, the direct optical resonances $|1\rangle \rightarrow |c\rangle$ and $|2\rangle \rightarrow |c\rangle$ are much weaker than those for mediated resonance pathes $|i\rangle \rightarrow |j\rangle \rightarrow |c\rangle$ (i = 1, 2 and j = 3, 4), so that the interaction between subbands $|j\rangle$ and the continuum and the influence of the direct transition $|i\rangle \rightarrow |c\rangle$ can be ignored[14]. Under these assumptions, following the standard process[24], the system dynamics can be described by equations for the density matrix elements in a rotating frame:

$$
\begin{aligned}
\dot\rho_{44} &= \mathrm{i}k\Omega_\mathrm{p}(\rho_{14}-\rho_{41}) + \mathrm{i}q\Omega_\mathrm{s}(\rho_{24}-\rho_{42}) - 2\gamma_4\rho_{44} + \gamma_{34}(\rho_{43}+\rho_{34}), &(1)\\
\dot\rho_{33} &= \mathrm{i}\Omega_\mathrm{p}(\rho_{13}-\rho_{31}) + \mathrm{i}\Omega_\mathrm{s}(\rho_{23}-\rho_{32}) - 2\gamma_3\rho_{33} + \gamma_{34}(\rho_{43}+\rho_{34}), &(2)\\
\dot\rho_{22} &= \mathrm{i}\Omega_\mathrm{s}(\rho_{32}-\rho_{23}) + \mathrm{i}q\Omega_\mathrm{s}(\rho_{42}-\rho_{24}) + \gamma_4\rho_{44} + \gamma_3\rho_{33} - 2\gamma_2\rho_{22} - \gamma_{34}(\rho_{43}+\rho_{34}), &(3)\\
\dot\rho_{43} &= -(\gamma_4+\gamma_3+\mathrm{i}\delta)\rho_{43} + \mathrm{i}\Omega_\mathrm{p}(k\rho_{13}-\rho_{41}) + \mathrm{i}\Omega_\mathrm{s}(q\rho_{23}-\rho_{42}) + \gamma_{34}(\rho_{44}+\rho_{33}), &(4)\\
\dot\rho_{42} &= -[\gamma_4+\gamma_2-\mathrm{i}(\Delta_2-\delta)]\rho_{42} - \mathrm{i}q\Omega_\mathrm{s}(\rho_{44}-\rho_{22}) + \mathrm{i}k\Omega_\mathrm{p}\rho_{12} - \mathrm{i}\Omega_\mathrm{s}\rho_{43} + \gamma_{34}\rho_{32}, &(5)\\
\dot\rho_{41} &= -[\gamma_4-\mathrm{i}(\Delta_1-\delta)]\rho_{41} - \mathrm{i}k\Omega_\mathrm{p}(\rho_{44}-\rho_{11}) + \mathrm{i}q\Omega_\mathrm{s}\rho_{21} - \mathrm{i}\Omega_\mathrm{p}\rho_{43} + \gamma_{34}\rho_{31}, &(6)\\
\dot\rho_{32} &= -(\gamma_3+\gamma_2-\mathrm{i}\Delta_2)\rho_{32} - \mathrm{i}\Omega_\mathrm{s}(\rho_{33}-\rho_{22}) + \mathrm{i}\Omega_\mathrm{p}\rho_{12} - \mathrm{i}q\Omega_\mathrm{s}\rho_{34} + \gamma_{34}\rho_{42}, &(7)\\
\dot\rho_{31} &= -(\gamma_3-\mathrm{i}\Delta_1)\rho_{31} - \mathrm{i}\Omega_\mathrm{p}(\rho_{33}-\rho_{11}) + \mathrm{i}\Omega_\mathrm{s}\rho_{21} - \mathrm{i}k\Omega_\mathrm{p}\rho_{34} + \gamma_{34}\rho_{41}, &(8)\\
\dot\rho_{21} &= -[\gamma_2-\mathrm{i}(\Delta_1-\Delta_2)]\rho_{21} - \mathrm{i}\Omega_\mathrm{p}\rho_{23} - \mathrm{i}k\Omega_\mathrm{p}\rho_{24} + \mathrm{i}\Omega_\mathrm{s}\rho_{31} + \mathrm{i}q\Omega_\mathrm{s}\rho_{41}, &(9)
\end{aligned}
$$

where $\Delta_1 = \omega_\mathrm{p} - \omega_{31}$ and $\Delta_2 = \omega_\mathrm{s} - \omega_{32}$ are the detunings of the optical fields with $\omega_{jk} = \omega_j - \omega_k$ (j,k = 1−4), where ω_j (j = 1−4) is the eigenfrequency of the state $|j\rangle$; δ is given by $\delta = \omega_4 - \omega_3$; the Rabi frequencies of the optical fields are defined by $\Omega_\mathrm{p} = \vec\mu_{13}\cdot\vec E_\mathrm{p}/2\hbar$ and $\Omega_\mathrm{s} = \vec\mu_{23}\cdot\vec E_\mathrm{s}/2\hbar$ respectively, where $\vec\mu_{13}$ and $\vec\mu_{23}$ are the dipole matrix elements; $k = \mu_{14}/\mu_{13}$ and $q = \mu_{24}/\mu_{23}$ present the ratios between the relevant subband transition dipole moments, and $\vec E_q$ (q = p, s) are the slowly varying amplitudes of the optical fields; the total electron decay rate $\gamma_i = \gamma_i^\mathrm{ph} + \gamma_i^\mathrm{deph}$ (i = 2, 3, 4) is the sum of the population decay originating from tunneling (γ_i^ph) and the dephasing rate (γ_i^deph)[14,23]. Equations (1)−(9) are constrained by $\sum\rho_{ii} \doteq 1$ (i = 1−4) and $\rho_{ij}^* = \rho_{ji}$. The values of parameters for this double QWs structure are $\gamma_4^\mathrm{ph} = 1.50$ meV, $\gamma_3^\mathrm{ph} = 1.58$ meV, $\gamma_2 = 2.36\times10^{-9}$ meV, $q\simeq0.88$, and $k\simeq-0.76$.

In the following, we aim at calculating the XPM between the signal and probe fields. In order to derive the linear and nonlinear susceptibilities, we need to obtain the steady-state solution of the density matrix equations. We consider the situation that the population is initially prepared in the ground subbands $|1\rangle$ and $|2\rangle$, and the probe and signal fields are very weak, i.e., $\rho_{11}^{(0)} + \rho_{22}^{(0)} = 1$ and $\Omega_\mathrm{p}, \Omega_\mathrm{s} \ll \Delta_\mathrm{p}, \Delta_\mathrm{s}$, and δ. Other initial population items are set to be zero, i.e., $\rho_{33}^{(0)} = \rho_{44}^{(0)} = 0$. Here, we originally considered the initial coherence. But we find, despite that initial coherence impacts third-order nonlinearity, it has no effect on the XPM. Therefore, we set the initial coherence to be zero. Thus, the first-order linear probe and signal susceptibilities are determined as

$$\chi_{\mathrm{p}}^{(1)} = \frac{2N\left|\mu_{13}\right|^2}{\hbar\varepsilon_0}\chi_p'^{(1)}, \tag{10}$$

$$\chi_{\mathrm{s}}^{(1)} = \frac{2N\left|\mu_{23}\right|^2}{\hbar\varepsilon_0}\chi_s'^{(1)}. \tag{11}$$

At the same time, the third-order cross phase modulated nonlinear susceptibility for the probe field is give by

$$\chi_{\mathrm{XPM}}^{(3)} = \frac{2N\left|\mu_{13}\right|^2\left|\mu_{23}\right|^2}{3\hbar^3\varepsilon_0}\chi_{\mathrm{XPM}}'^{(3)}. \tag{12}$$

In Eqs. (10)−(12), N is the electron volume density, $\chi_{\mathrm{p}}'^{(1)}$, ${\chi_{\mathrm{s}}}'^{(1)}$, and $\chi_{\mathrm{XPM}}'^{(3)}$ are expressed as

$$\chi_{\mathrm{p}}'^{(1)} = -\frac{(\Delta_1-\delta+\mathrm{i}\gamma_4)+k^2(\Delta_1+\mathrm{i}\gamma_3)+2\mathrm{i}k\gamma_{34}}{(\Delta_1-\delta+\mathrm{i}\gamma_4)(\Delta_1+\mathrm{i}\gamma_3)+\gamma_{34}^2}\rho_{11}^{(0)}, \tag{13}$$

$$\chi_{\mathrm{s}}'^{(1)} = -\frac{[\Delta_2-\delta+\mathrm{i}(\gamma_4+\gamma_2)]+q^2[\Delta_2+\mathrm{i}(\gamma_3+\gamma_2)]+2\mathrm{i}q\gamma_{34}}{[\Delta_2-\delta+\mathrm{i}(\gamma_4+\gamma_2)][\Delta_2+\mathrm{i}(\gamma_3+\gamma_2)]+\gamma_{34}^2}\rho_{22}^{(0)}, \tag{14}$$

and

$$\begin{aligned}\chi_{\mathrm{XPM}}'^{(3)} = {} & \frac{(\Delta_1-\delta+\mathrm{i}\gamma_4+\mathrm{i}k\gamma_{34})[(2B_{33}+B_{44}+B_{22})-B_{21}+k(B_{43r}-\mathrm{i}B_{43i})]}{(\Delta_1-\delta+\mathrm{i}\gamma_4)(\Delta_1+\mathrm{i}\gamma_3)+\gamma_{34}^2} \\ & +\frac{[k\cdot(\Delta_1+\mathrm{i}\gamma_3)+\mathrm{i}\gamma_{34}]\cdot[k\cdot(2B_{44}+B_{33}+B_{22})-qB_{21}+(B_{43r}+\mathrm{i}B_{43i})]}{(\Delta_1-\delta+\mathrm{i}\gamma_4)(\Delta_1+\mathrm{i}\gamma_3)+\gamma_{34}^2},\end{aligned} \tag{15}$$

with

$$\begin{cases} A_{31} = -\dfrac{\Delta_1-\delta+\mathrm{i}\gamma_4+\mathrm{i}k\gamma_{34}}{(\Delta_1-\delta+\mathrm{i}\gamma_4)(\Delta_1+\mathrm{i}\gamma_3)+\gamma_{34}^2}\cdot\rho_{11}^{(0)}, \\ A_{41} = -\dfrac{k(\Delta_1+\mathrm{i}\gamma_3)+\mathrm{i}\gamma_{34}}{(\Delta_1-\delta+\mathrm{i}\gamma_4)(\Delta_1+\mathrm{i}\gamma_3)+\gamma_{34}^2}\cdot\rho_{11}^{(0)}, \\ A_{32} = -\dfrac{\Delta_2-\delta+\mathrm{i}(\gamma_4+\gamma_2)+\mathrm{i}q\gamma_{34}}{[\Delta_2-\delta+\mathrm{i}(\gamma_4+\gamma_2)][\Delta_2+\mathrm{i}(\gamma_3+\gamma_2)]+\gamma_{34}^2}\cdot\rho_{22}^{(0)}, \\ A_{42} = -\dfrac{q[\Delta_2+\mathrm{i}(\gamma_3+\gamma_2)]+\mathrm{i}\gamma_{34}}{[\Delta_2-\delta+\mathrm{i}(\gamma_4+\gamma_2)][\Delta_2+\mathrm{i}(\gamma_3+\gamma_2)]+\gamma_{34}^2}\cdot\rho_{22}^{(0)}, \end{cases} \tag{16}$$

$$\begin{cases} B_{21} = \dfrac{\mathrm{Re}[A_{32}]-\mathrm{i}\mathrm{Im}[A_{32}]+k(\mathrm{Re}[A_{42}]-\mathrm{i}\mathrm{Im}[A_{42}])-A_{31}-qA_{41}}{\Delta_1-\Delta_2+\mathrm{i}\gamma_2}, \\ B_{43r} = \dfrac{\delta(q\mathrm{Re}[A_{32}]-\mathrm{Re}[A_{42}])+(\gamma_4+\gamma_3)[(1+\frac{q\gamma_{34}}{\gamma_4})\mathrm{Im}[A_{42}]+q(1+\frac{\gamma_{34}}{\gamma_3})\mathrm{Im}[A_{32}]]}{(\gamma_4+\gamma_3)^2(1+\frac{\gamma_{34}^2}{\gamma_4\gamma_3})+\delta^2}, \end{cases} \tag{17}$$

$$B_{43i} = \frac{q\mathrm{Re}[A_{32}]-\mathrm{Re}[A_{42}]+\delta B_{43r}}{\gamma_4\gamma_3}, \quad B_{44} = \frac{q\mathrm{Im}[A_{42}]+\gamma_{34}B_{43r}}{\gamma_4}, \quad B_{33} = \frac{\mathrm{Im}[A_{32}]+\gamma_{34}B_{43r}}{\gamma_3}, \tag{18}$$

$$B_{22} = \frac{-\mathrm{Im}[A_{32}]-q\mathrm{Im}[A_{42}]+\gamma_{34}B_{43r}}{2\gamma_2}. \tag{19}$$

$\mathrm{Im}[\chi_{\mathrm{p}}'^{(1)}]$ and $\mathrm{Re}[\chi_{\mathrm{p}}'^{(1)}]$ account for the linear probe absorption and dispersion respectively. Comparing Eqs. (13) and (14) with the expression of the susceptibility in EIT[25], it is easy to find that, in our structure, the role of the coupling field is replaced by tunneling. At the same time, $k<0$ indicates a destructive interference in linear absorption. In Fig. 2, we plot their evolution versus the probe detuning Δ_1 with arbitrary value of $\rho_{11}^{(0)}\neq 0$. From the figure, we can see that the absorption is the minimum approximating to zero with positive dispersion at $\Delta_1 = 6.65$ meV and TIT appears. Similar results can be obtained for the signal field, i.e., the linear signal absorption is the minimum approximating to zero with positive dispersion at $\Delta_2 = 6.65$ meV, which can be deduced from Eqs. (13) and (14). The group velocity of the probe and signal fields are described as

$$v_{\mathrm{g}}^j = \frac{c}{n_j+\omega_j(\mathrm{d}n_j/\mathrm{d}\omega_j)}\ (j=\mathrm{p},\mathrm{s}), \tag{20}$$

where

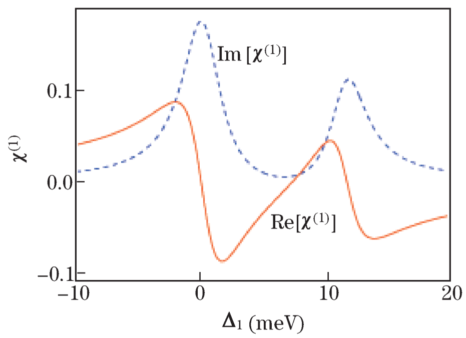

Fig. 2. Spectra of absorption and dispersion of the probe field with arbitrary value of $\rho_{11}^{(0)} \neq 0$.

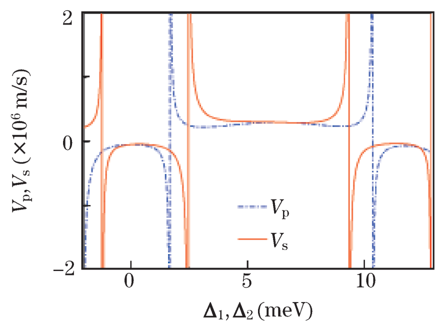

Fig. 3. Velocities of the probe and signal fields, V_p and V_s, versus probe detuning Δ_1 and signal detuning Δ_2, respectively.

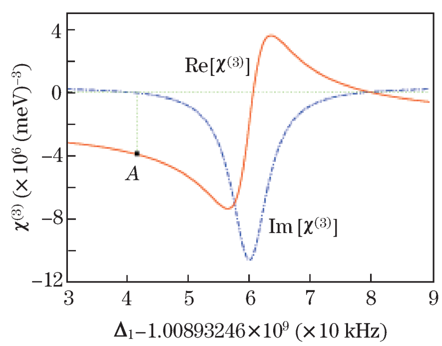

Fig. 4. $\mathrm{Im}[\chi'^{(3)}_{\mathrm{XPM}}]$ and $\mathrm{Re}[\chi'^{(3)}_{\mathrm{XPM}}]$ versus the probe detuning Δ_1.

$$n_j = \sqrt{1 + \mathrm{Re}[\chi_j^{(1)}]}\ (j = \mathrm{p}, \mathrm{s}). \qquad (21)$$

It is well known that the condition of group velocity matching between the probe and signal fields is of fundamental importance for achieving a large XPM, which is necessary for their effective interaction length. In our structure, we pursue the coherent manipulation in the regime of TIT which could result in a dramatic reduction of the group velocity of the weak propagating fields accompanied by vanishing absorptions. In order to match the group velocities $v_\mathrm{g}^\mathrm{p} = v_\mathrm{g}^\mathrm{s}$ in the transparent window, the initial population should be prepared as $\rho_{11}^{(0)} = 0.35$ and $\rho_{22}^{(0)} = 0.65$. For clarity, we plot the evolutions of v_g^p versus the probe detuning Δ_1 and v_g^s versus the signal detuning Δ_2 for $\rho_{11}^{(0)} = 0.35$ and $\rho_{22}^{(0)} = 0.65$ in Fig. 3. It is obvious that at the point $\Delta_1 = \Delta_2 = 6.65$ meV, two group velocities are matched, i.e., $v_\mathrm{g}^\mathrm{p} = v_\mathrm{g}^\mathrm{s}$.

Successively, we explore the third-order Kerr effect on the basis of the matched group velocities. In our structure, owing to resonant tunneling, the wave functions of subbands $|3\rangle$ and $|4\rangle$ are symmetric and anti-symmetric combinations of $|\mathrm{se}\rangle$ and $|\mathrm{de}\rangle$ (Fig. 1), which leads to $qk < 0$ and constructive interference in XPM nonlinearity. This result can be analogized from Ref. [14] or discerned from the expatiatory expression by substituting Eqs. (13), (14), and (16)−(19) into Eq. (15). Besides, due to the weak mechanical cross between wave functions of two low-lying subbands $|1\rangle$ and $|2\rangle$ (Fig. 1), the dipole transition is very weak, which inevitably results in a small dipole matrix element μ_{12} and then a small transition rate γ_2[16]. The small transition rate could help to produce giant XPM that can be seen from Eq. (15). With $\Delta_2 = 6.65$ meV, we plot the evolutions of $\mathrm{Im}[\chi'^{(3)}_{\mathrm{XPM}}]$ and $\mathrm{Re}[\chi'^{(3)}_{\mathrm{XPM}}]$ in Fig. 4, which respectively account for two-photon absorption and XPM, versus the probe detuning Δ_1 in the TIT window, i.e., close up to the transparent point $\Delta_1 = 6.65$ meV. Here, in the figure, we transfer the unit of Δ_1 from meV to 10 kHz for clarity. Obviously, within the transparency window, both strengths of XPM and two-photon absorption are enhanced largely. While, for certain probe detuning, for example, at the point A [$\Delta_1 = (1.00893246 \times 10^9 + 4.1) \times 10$ kHz], it is fortunate that the strength of XPM is very large ($\mathrm{Re}[\chi'^{(3)}_{\mathrm{XPM}}] = -3.91 \times 10^6$ (meV)$^{-3}$) accompanied with the two-photon absorption being vanished. This suggest that, in our structure, giant enhanced XPM can be achieved with vanishing linear and nonlinear absorptions simultaneously. This interesting result is produced by the combination of a destructive interference in linear absorption with a constructive interference in the nonlinear susceptibility associated with XPM, which is induced by resonant tunneling. It is necessary to point out that the narrow probe frequency input corresponding to the point A in Fig. 4 can be realized by using frequency comb.

In information processing, if a large single-photon nonlinear phase shift π arising from such a Kerr effect was achieved, it can be used to implement two-qubit quantum logic gates. Here, the phase shift of the probe filed is calculated. In our structure, for two matched Gaussian pulses, the nonlinear phase shift can be determined from the slowly varying envelope equation[17]. With peak signal Rabi frequency $\Omega_\mathrm{s}^\mathrm{peak}$ which can be derived from the relation of electric field and power density[15], the nonlinear cross-phase shift of the probe field can be written as

$$\Phi_{\mathrm{XPM}} = \frac{N|\mu_{13}|^2 \omega_\mathrm{p} l |\Omega_\mathrm{s}^\mathrm{peak}|^2}{3\hbar\varepsilon_0} \mathrm{Re}[\chi'^{(3)}_{\mathrm{XPM}}]. \qquad (22)$$

Numerical findings indicate that, this semiconductor QWs structure (point A) could produce π XPM phase shift with focusing only one single photon into an area of 1 μm^2 (the intensity of a single photon per nanosecond on area of 1 μm^2 is $\sim$ 1.6 mW/cm^2) by counting in the proper electron volume density ($N = 4 \times 10^{11}$ cm^{-2}) and interaction length (50 cycles). Compared with the results about XPM in quantum information, it realizes π XPM phase shift at the single-photon level in semiconductor.

In conclusion, we have studied the linear and nonlinear properties in an asymmetric AlGaAs/GaAs double QWs structure. In this semiconductor structure, under the condition of group velocity matching, giant Kerr nonlinearity associated with XPM can be achieved with vanishing both the linear and two-photon absorptions. Furthermore, we realize π XPM phase shift under the single-photon level, which is desirable to implement two-qubit quantum logic gates. The essence is the constructive interference in nonlinear susceptibility associated with XPM induced by resonant tunneling in combination with TIT.

This work was supported by the National Natural Science Foundation of China (Nos. 60708008 and 10734080), the Project of Academic Leaders in Shanghai (No. 07XD14030), and the Knowledge Innovation Program of the Chinese Academy of Sciences.

References

1. H. Schmidt and A. Imamoğlu, Opt. Lett. **23,** 1007 (1998).
2. H. Li, J. Liu, C. Wang, G. Ni, R. Li, and Z. Xu, Chin. Opt. Lett. **5,** S129 (2007).
3. L. Wang, K. Xia, H. Sun, Y. Niu, and S. Gong, Chin. Opt. Lett. **5,** S126 (2007).
4. R. W. Boyd, *Nonlinear Optics* (Academic, San Diego, 1992).
5. M. A. Nielsen and I. L. Chuang, *Quantum Computation and Quantum Information* (Cambridge University Press, Cambridge, 2000).
6. H. Schmidt and A. Imamoğlu, Opt. Lett. **21,** 1936 (1996).
7. T. Nakajima, Opt. Lett. **25,** 847 (2000).
8. M. C. Phillips, H. Wang, I. Rumyantsev, N. H. Kwong, R. Takayama, and R. Binder, Phys. Rev. Lett. **91,** 183602 (2003).
9. H. Schmidt, K. L. Campman, A. C. Gossard, and A. Imamoğlu, Appl. Phys. Lett. **70,** 3455 (1997).
10. J.-H. Wu, J.-Y. Gao, J.-H. Xu, L. Silvestri, M. Artoni, G. C. La Rocca, and F. Bassani, Phys. Rev. Lett. **95,** 057401 (2005).
11. C.-H. Yuan and K.-D. Zhu, Appl. Phys. Lett. **89,** 052115 (2006).
12. H. Sun, S. Gong, Y. Niu, S. Jin, R. Li, and Z. Xu, Phys. Rev. B **74,** 155314 (2006).
13. H. Sun, Y. Niu, R. Li, S. Jin, and S. Gong, Opt. Lett. **32,** 2475 (2007).
14. U. Fano, Phys. Rev. **124,** 1866 (1961).
15. A. Steane, Rep. Prog. Phys. **61,** 117 (1998).
16. S. E. Harris and Y. Yamamoto, Phys. Rev. Lett. **81,** 3611 (1998).
17. D. Petrosyan and Y. P. Malakyan, Phys. Rev. A **70**, 023822 (2004).
18. C. Ottavian, S. Rebić, D. Vitali, and P. Tombesi, Eur. Phys. J. D **40,** 281 (2006).
19. M. Fleischhauer, A. Imamoglu, and J. P. Marangos, Rev. Mod. Phys. **77,** 633 (2005).
20. Z.-B. Wang, K.-P. Marzlin, and B. C. Sanders, Phys. Rev. Lett. **97,** 063901 (2006).
21. C. Ottaviani, D. Vitali, M. Artoni, F. Cataliotti, and P. Tombesi, Phys. Rev. Lett. **90,** 197902 (2003).
22. I. Fushman, D. Englund, A. Faraon, N. Stoltz, P. Petroff, and J. Vučković, Science **320,** 769 (2008).
23. J.-H. Wu, J.-Y. Gao, J.-H. Xu, L. Silvestri, M. Artoni, G. C. La Rocca, and F. Bassani, Phys. Rev. A **73,** 053818 (2006).
24. S. E. Harris, Phys. Rev. Lett. **62,** 1033 (1989).
25. M. O. Scully and M. S. Zubairy, *Quantum Optics* (Cambridge University Press, Cambridge, 1997).